OPEN ACCESS

International
Journal
Of Modern Engineering Research (IJMER)

Finite Element Modeling of Tool Stresses in Hard Turning of AISI L2 Steel: Prediction by ANN

Mehmet Erdi Korkmaz[1*] Mustafa Günay[2]
[1]*Mechanical Engineering Department, Karabük University, Turkey*
[2]*Mechanical Engineering Department, Karabük University, Turkey*

ABSTRACT: *Hard turning is a finishing process like grinding involving many cutting conditions, namely, depth of cut, feed rate, cutting speed, tool material and tool geometry, etc. Tool nose radius which is one of these cutting conditions influences surface finish and productiveness in hard turning process. In this study, resultant cutting force (F_R) and equivalent (von Mises) stress depending on cutting conditions (tool nose radius, cutting speed, depth of cut and feed rate) were investigated in hard turning of AISI L2 steel using TiN coated mixed ceramic inserts. The hard turning experiments were conducted subjected to the experimental design. The distributions of cutting tools stress were analyzed statically based on finite element method by using ANSYS software and ANN. When comparing FEA and ANN results, reliability of neural network model was confirmed based on statistical error control methods. ANOVA results showed that the most significant factor on F_R is depth of cut while cutting speed has insignificant effect. FEA results showed that the boundary conditions for loading of cutting forces are correct and the prediction of cutting tool stresses statically by finite element analysis can be determined in hard tuning processes.*

Keywords: *ANN, Cutting force, FEA, Hard turning, Tool stress*

I. INTRODUCTION

Manufacturing of hardened steel elements with high precision and surface quality is widely provided by grinding. Hard machining has been proposed to partly replace grinding because of its comparatively high cost. Flexibility and positive environmental effect are another benefits of dry hard machining[1]. Additionally, surfaces by hard turning can have a longer fatigue life when compared with grinding parts[2].

Recently, machining of hardened steel is a subject of concern for industrial fabrication and technical investigation as it presents a quantity of probable benefits, involving high accuracy, lower tooling cost, shorter setup time, less process step, flexibility of larger part geometry, and generally the usage of cutting fluid is unrequired during turning of hardened steels. Manufacturing costs are expected to be reduced by up to 30% once hard turnıng is used for producing difficult part[3]. Moreover, the main concerns of hard turning are cost of tool materials and the effect of the process on machinability characteristic. The machining of hardened steel using polycrystalline cubic bore nitrite and ceramic tool[4] is commonly known as a best replacement to costly grinding operation[5]. On the other hand, Aouici et al.[6] mentioned about the optimization of cutting conditions to decrease the cost in mass production. For this purpose, authors performed an optimization study in hard turning of H11 tool steel with CBN insert by using response surface methodology.

The result shows that components of cutting force are affected primarily from depth of cut and workpiece hardness. Many investigations have been performed to research the performance of carbide and ceramic tool in cutting of several hardened materials due to higher cost of CBN. Gaitonde et al.[7] studied effect of cutting depth and machining time on machning force, power, surface roughness and tool wear have been determined in hard turning of D2 steel with CC650, CC650WG and GC6050WH ceramic tools. According to experimental results, the machining force and power rise with increasing depth of cut while tool wear decreases with increasing depth of cut. Chinchankar and Choudhury[8] investigated on performance of coated carbide tool considering influences of workpiece hardness and cutting parameters in turning of hardened AISI 4340 steel. ANOVA results revealed that cutting forces were influenced primarily by depth of cut followed by feed rate. Also, authors emphasized that coated carbide tools can be used in different ranges of cutting speed at lower feed rate and depth of cut. Karpuschewski et al.[9] observed that combinational effects of cutting edge preparation and coating decrease significantly friction force in scratch test, a factor responsible for decreasing the force when hard turning with ceramic tool. Hence, the authors emphasized that there is very insignificant change of microhardness of coated and uncoated ceramics. In finish hard machining with coated ceramics, Sokovic et al.[10] analyzed the tribological and cutting properties of different coating of deposited with PVD and CVD technique

on Al2O3/SiC ceramic inserts. The result shows that there is no direct relationship between the coating types and machining result. The smallest flank wear was obtained with insert of two layers coating, but the best surface finish was produced by multilayer coating. Bhattacharya et al.[11] studied on the cutting performance of surface modified Al2O3/TiOC mixed ceramic cutting tools. The authors has modified the inserts by post treatment under argon/CO2 atmosphere to form a TiN layer with thickness of 1–1.5 μm. It was proved that the surface modified tools have higher performance with 29% than sintered tools in respect of wear rate.

Experimental methods have many difficulties in the cutting process for analysis of factors, namely, cutting force, temperature, strain, strain rate, and stress. Thus, the mathematical model predicting these factors has been established to increase the production capability uncompromising their required values. The techniques such as regression analysis, finite element method, fuzzy logic and artificial neural network etc. are used. These modelling studies have been performed to decrease the experimental costs and predetermine the relationships between cutting parameters and machining outputs[12]. FEM is the most commonly used among these techniques in order to forecast the machining outputs and characteristics of the machining process. Thus, this paper focused on finite element modelling applied to forecast stresses on cutting tools statically while cutting forces were found experimentally in turning of hardened AISI L2 steel used for manufacturing industries about circular saws for timber, saws for nonferrous, machine saws, measuring tools, tools such as knives, punches, guide rods, twist drills, reamers. Finally, artificial neural network (ANN) analysis has been used for mathematical modelling of machining outputs such as cutting forces and stresses. Many modelling research[13,14] have been studied dynamically for the performance of different tool grade in the cutting process of various materials. Yan et al.[15] investigated the effects of strain, strain rate and temperature on flow stress in hard turning of H13 mold steel. It is claimed that the determination of mechanical behavior of flow stresses is very difficult in hard turning and so this problem should be solved with finite element method. Authors emphasized the validity of finite element model with DEFORM 2D when compared with experimental data. Umbrello et al.[16] studied on flow stresses depending on hardness for numerical simulations in hard turning of H13 with different cutting speed and depth of cut. It was stated that cutting tool stress decreases with increasing cutting speed, but the stress increases with increasing material hardness. It is noticed that the results are very similar while comparing of data taken from experiments and finite element analysis with DEFORM. Özel[17] investigated the effects of cutting tool geometries on cutting force, stress and tool wear in hard turning of AISI 4340 with PCBN cutting tool and then developed a model with the help of 3D finite element method. It is observed that variable edged cutting tool is more useful than that of uniform edged.

These cutting tools provide longer tool life and less consumption of power. It is proved that the finite element model with DEFORM 3D and experimental results are very similar and so the model has high validity. Özel and Nadgir[18] has obtained thrust and main cutting forces in the result of hard turning experiments on H13 steel with CBN tool by using different levels of cutting speed, feed rate and cutting time. Some of these experimental data have been separated for training and some for testing in ANN modelling. An error with 15.09% has been determined between real and modelling values when analyzing the model with single hidden layer. Authors indicate that the model can be applicable although this error is not too little. Based on experiments in hard turning of AISI 52100 with PCBN tool performed by Umbrello et al.[19], the effects of cutting parameters on residual stresses have been examined. A mathematical model with ANN has been developed with the help of experimental data. An error with 4-10% has been observed between real and modelling values when analyzing whole data in this ANN modelling with three layer and the validity of this model has been emphasized. Wang et al.[20] investigated the effects on the tool wear of cutting parameters in hard turning of H13 steel with CBN tool. An ANN model with single hidden layer has been developed based on experiments by using four different cutting parameters. The authors found that there is a 12.81% error when compared experimental and modelling values and so the model can be applicable. These studies contain modelling of cutting tool stresses dynamically based on finite element method in hard turning. This method is of course applicable with high accuracy but it takes very long time because the analyses are performed with dynamic solution. Nowadays, static solutions are developed by finite element methods with less time and high accuracy. Kurt et al.[21] developed a finite element model for determining the cutting tool stress in finish turning of H13 with ceramic tools. The results show that cutting tool stresses decrease with increasing tool chip contact area. Also, the authors emphasized that the areas of stress concentration in FEA provide information about probable tool wear type once finish turning has been continued. Thus, it is deduced that the probable crater wear can arise at tip of tool chip contact area because of high compression stresses once finish turning has been continued.

There is a little if any studies on modeling of cutting tool stress statically in hard turning although there is a lot of modelling studies dynamically on hard turning as can be understood from mentioned literature. In this study, firstly the changes of cutting forces depending on cutting conditions (tool nose radius, cutting speed, depth of cut and feed rate) has been investigated during the machining of AISI L2 steel (60±1 HRC) with the coated mixed ceramic inserts. Secondly, the stresses distribution on cutting tools was analyzed statically based

on finite element method by using ANSYS. Finally, a mathematical model via artificial neural network has been developed for predicting equivalent/von Mises stress (S_{EQV}) which has significant effect on cutting tool wear.

II. MATERIAL AND METHOD

2.1. Experimental Procedure

The purpose of this study was investigating the effects of cutting parameters on cutting forces and cutting tool stresses in hard turning of AISI L2 steel using ceramic tools. Hard turning experiments were carried out using CNC lathe with 20 HP spindle power. These cutting conditions were used for the experiments: cutting depth (a) of 0.1, 0.2 and 0.3 mm, feed rate (f) of 0.05–0.10 and 0.15 mm/rev, cutting speed (V) of 90, 120 and 150 m/min, and tool nose radius (r) of 0.4, 0.8 and 1.2 mm. However, cutting force components which are main cutting force_F_c, feed force_F_f and radial force_F_r were also added as cutting parameters in order to analyze von Mises stress. The workpiece material is AISI L2 steel with this chemical composition: 1.10-1.25 % C, 0.15-0.30 % Si, 0.20-0.40 % Mn, 0.50-0.80 % Cr, 0.07-0.12 % V, 0.03 % P, 0.03 % S and the rest is Fe. The workpieces were hardened to 60±1 HRC by means of heat treatments (quenching in a vacuum atmosphere).

TiN coated (DNGA 150604 S01525) ceramic insert with three different tool nose radius was used to turning of L2 tool steel. The insert was fixed to a toolholder of PDJNR 2525M15. Combinations of the inserts and toolholder resulted in effective rake angle γ=-31°, clearance angle α=-6°, cutting edge inclination angle λ=-6° and approaching angle χ_r=93°. The workpiece was clamped into the machine to minimise runout and maximize rigidity. Measurements of the cutting forces were achieved by the Kistler pizoelectric dinamometer Type 9257B connected to serial of multichannel charge amplifier types Kistler 5070A. The measured values were continuously monitored and recorded throughout the Dynoware software.

2.2. FEA for the Cutting Tool

The finite element analyses of the tool stress were performed with ANSYS Workbench software depending on finite element method. 3D model of the cutting tools (cutting tool and toolholder), defining of materials property requisite for cutting tool, element types and its size, meshing of the model, designation of boundary and loading conditions, and selecting of solution methodology are preparations required for the analyses, respectively. After the cutting tools are modelled via SolidWorks, the prepared solid models were imported to ANSYS Workbench. Moreover, the tool–chip contact area was determined in the modeling of the cutting tools based on Zorev approach[22] and applied as in the literature[18]. The tool-chip contact length shown in Fig. 1 is calculated as follow[23]:

$$l_c = 2 \cdot \lambda \cdot a \qquad (1)$$

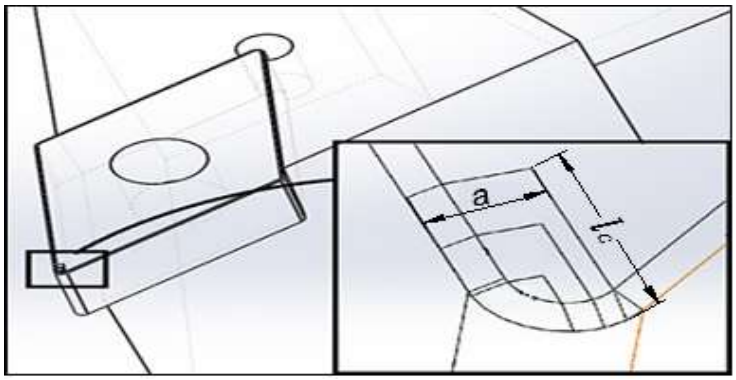

Figure 1 Tool-chip contact length and area

Where, l_c, a and λ are the tool–chip contact length, the undeformed chip thickness, the coefficient of chip thickness, respectively. The coefficient of chip thickness is the ratio of a_1 (the chip thickness) to a. The values of a_1 have been measured from hard turning as 0.18, 0.36, 0.54 mm for depth of cut a=0.1, 0.2, 0.3 mm, respectively. According to Toropov and Ko with Eq. 1, the tool–chip contact areas (Fig. 1) with l_c=0.36, 0.72, 1.08 mm were occurred on tool rake face for each depth of cut, respectively. In addition, some details for the tool holder were created like small edge chamfering/rounding on toolholder and clamping parts, and also the parts of toolholder in the dynamometer were ignored to decrease the number of element and calculation times in finite element method (FEM) modelling. The tool holder was modelled depending on actual clamping length in turning. The material property such as elasticity module (E) and Poisson ratio (ν) in modelling of cutting tools are used for linear elastic material models (Table 1). The values of E and ν for the coated ceramic tool and toolholder were used as Ref.[24]. Moreover, C3D10 (10-node quadratic tetrahedral element) was used as the

element type for the cutting tools in the FEM. The meshing was performed by considering the default values suggested from ANSYS Workbench. The meshes were applied to tool chip contact area on insert rake face densely and to other part of the cutting tool rarely (Fig. 2a). Consequently, the total 37759, 42664 and 52968 nodes were used while 21554, 24881 and 31942 elements were used for cutting tools that of 0.4, 0.8 and 1.2 mm tool nose radius in the analysis, respectively. The behaviour of contact surfaces should be considered in FEM, although the contacts in the model were automatically perceived. Then, the contact surfaces are bonded symmetrically in all directions. Hence, the additional force for clamping the insert with the tool holder is not required.

Table 1 The material properties of cutting tool and tool holder [24].

Cutting tools	***E* (GPa)**	***ν***
Tool holder	210	0.28
Coated ceramic insert	600	0.25

The designation of the boundary and loading conditions is the final preparation step before the solution for FEM modelling. For this purpose, the cutting force components (F_c, F_f, F_r) affecting on the insert are applied to the tool–chip contact area depending on the following processes: The main cutting force (F_c) was applied to tool chip contact area as triangular variable load. Here, the F_c value is zero at tip of the tool chip contact area based on coordinate system origin shown in Fig. 2b. Here, the chip is presumed as curled and removed from rake face. Besides, the highest F_c value at the first contact point between the insert and chip at distance lc in Z direction is shown in Fig. 2b. However, the radial force (F_r) and feed force (F_f) were applied straight to the tool chip contact area in X and Y directions whose are radial and feed motion of cutting tool, respectively. The weights of the cutting tools, the vibration and temperature occurred in hard machining were ignored in FEA to diminish the calculation time in analyses.

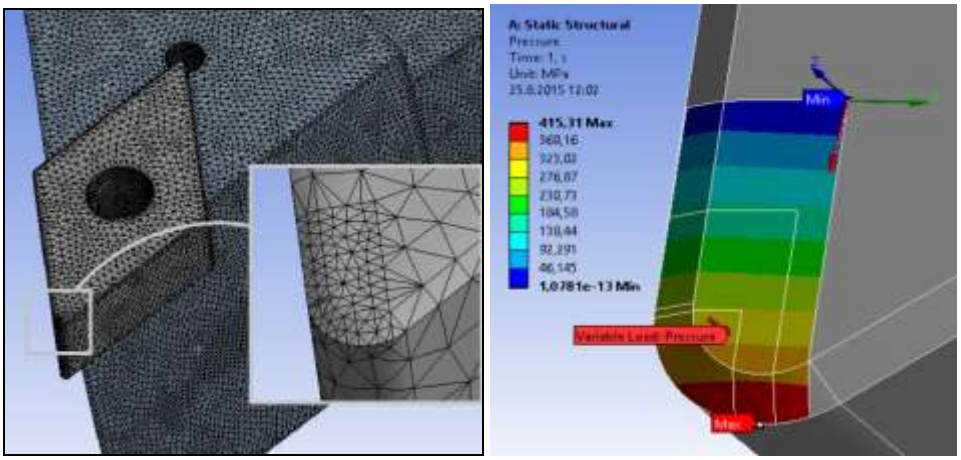

a) **b)**

Figure 2 The meshing and loading; a) Mesh structure, b) Loading of F_c

Finally, FEM solution was performed by ANSYS Workbench software as nonlinear because of the contact surfaces between cutting tool and toolholder. The converge criterion controls the relation between force and displacement with Full Newton-Raphson method in each iterative solution step in the FEA. Wear area or wear form on cutting tool may be forecasted according to distributions of von Mises stresses. Therefore, the results of von Mises stress (S_{EQV}) were examined for the detection of possible wear zone of the cutting tool according to the cutting conditions.

2.3. ANN Analysis For Cutting Tool Stress

ANN consisting of inputs by users and an output reflecting the information kept in connections during training is a nonlinear system involving neurons and weighted connection links. A multilayer ANN involves at least three layer, namely, input, hidden and output layers demonstrated in Fig. 3. The referred learning or training is reached by decreasing the sum of square error between the predicted output of ANN and the actual output from training data, by continuously adjusting and lastly defining the weights that connects neurons in conjunctive layers[25].

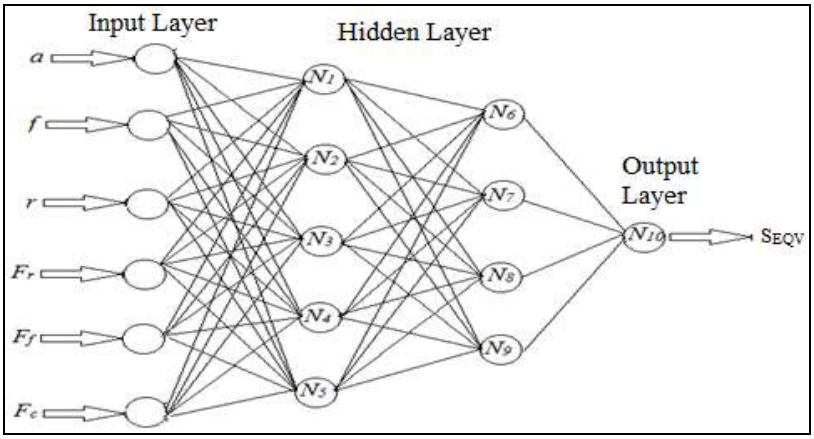

Figure 3 The network topology for von Mises stress (S_{EQV})

ANN analyses were performed for S_{EQV} values in 27 results of finite element analysis that are nine results for each tool nose radius. Depth of cut, feed rate, tool nose radius, radial force, feed force and main cutting force values were entered as independent parameters (inputs) and S_{EQV} values were entered as dependent parameter (output) in ANN software program. 6 results of FEA have been chosen for testing (confirmation) and rest of 21 results have been used as training data in software program. Many trials have been done in order to specify the most suitable topology by examining six inputs and one output in data set. The most appropriate topology has been determined as 6-5-4-1 in modeling of von-Mises stresses with ANN (Fig.3). It was stated that two level hidden layer should be applied and the number of neurons should be chosen as nine. As a result, N1, N2, N3, N4, N5 neurons and N6, N7, N8, N9 neurons have been determined as first level and second level in hidden layers, respectively. N10 is output neuron of network.

The weights of each neurons have been specified in training result and average deviation value has been calculated from ANN output values and FEA results. Output neuron developed for estimated von-Mises stresses has been calculated by using Fermi transfer function.

$$E_{i10} = \frac{1}{1+e^{-4(\sum_i^n w_i N_i - 0{,}5)}} \tag{2}$$

Here, n and wi show the number of neurons used in hidden layer and weights of neurons, respectively. Ni is the effect on S_{EQV} of each neuron used in hidden layer. According to input parameters in ANN model;

$$E_i = 4 \cdot (c_{1i} \cdot a + c_{2i} \cdot f + c_{3i} \cdot r + c_{4i} \cdot F_r + c_{5i} \cdot F_f + c_{6i} \cdot F_c - 0{,}5) \tag{3}$$

$$N_i = \frac{1}{1+e^{-E_i}} \tag{4}$$

Were defined. Cij constants show the weight of each neuron used in hidden layer after the result of data training set in Pythia program. While Cij values have six and five constants in first and second layer, respectively, those have been given in Table 2.

Table 2 Weights of each neurons for S_{EQV}

i	C_{1i}	C_{2i}	C_{3i}	C_{4i}	C_{5i}	C_{6i}
First level neurons						
1	-0.740696	0.417299	-0.343089	-0.079624	0.918361	1.021702
2	1.352316	0.876483	0.633232	-1.21453	-0.925163	-0.070125
3	1.135177	-0.272836	1.049628	-0.619835	0.514685	0.526775
4	0.707695	0.295807	0.925856	-0.438958	1.02607	0.408586
5	-1.489151	0.421879	0.623488	-0.097755	0.69342	-0.316462
Second level neurons						
6	0.463132	1.605703	-0.178795	-0.819613	-1.590196	
7	-0.509779	-0.40531	0.835566	-0.7476	0.911726	
8	-0.423949	-0.620749	0.627712	-0.195197	0.387887	
9	0.928654	-0.914612	-0.461825	-0.000804	0.453421	

In the network topology, Eqn. 5 is used for first level neurons (N1, N2, N3, N4, N5) and Eqn. 6 is used for second level neurons (N6, N7, N8, N9) because of two-level hidden layer in S_{EQV}. The output neuron of network for prediction model developed according to input parameters was achieved by Fermi function with Eqn. 7. Finally, the prediction model of S_{EQV} was obtained with Eqn. 8.

$$E_{i1-5} = w_{1i} \cdot a + w_{2i} \cdot f + w_{3i} \cdot r + w_{4i} \cdot F_r + w_{5i} \cdot F_f + w_{6i} \cdot F_c \quad (5)$$

$$E_{i6-9} = w_{i6} \cdot N_1 + w_{i7} \cdot N_2 + w_{i8} \cdot N_3 + w_{i19} \cdot N_4 \quad (6)$$

$$E_{i10} = \frac{1}{1+e^{-4(-0{,}821717 \cdot N_6 + 2{,}009181 \cdot N_7 + 2{,}030742 \cdot N_8 + 1{,}845182 \cdot N_9}} \quad (7)$$

$$S_{eqv} = E_{i10} \cdot \left(S_{eqv_{max}} - S_{eqv_{min}}\right) + S_{eqv_{min}} \quad (8)$$

III. RESULTS AND DISCUSSION

3.1. Evaluation of Resultant Force

The main cutting force is most important factor with respect of energy consumption in turning processes. However, the magnitude order of cutting force components (F_f, F_r, F_c) can change due to especially tool geometry, cutting parameters and material hardness in hard turning. Therefore, resultant force/machining force (F_R) should be taken into account for the analysis of cutting forces in respect of cutting tool stresses, which affect the tool wear indirectly. The resultant force is determined from following equation:

$$F_R = \sqrt{F_c^2 + F_f^2 + F_r^2} \quad (9)$$

F_R values have been calculated from measured cutting force components by Eqn. 9. The change of F_R values obtained with three different tool nose radius according to cutting depth, feed and cutting speed was given in Fig 4.

It is known that cutting tool geometry is an important factor affecting chip formation and then cutting forces positively or negatively. Therefore, the effects of tool nose radius on resultant forces were assessed with the help of figures. It was determined that F_R values increased about 39 % with increasing of nose radius from 0.4 to 1.2 mm in the lightest cutting condition (a= 0.1mm, f=0.05 mm/rev). It is observed that the change in resultant force values is similar for three different tool nose radius. Resultant force increases with increasing depth of cut and feed rate for all tool nose radius (as seen Fig. 4). The highest value for resultant force in nose radius of 0.4 mm is calculated as 288.68 N for the cutting speed of 120 m/min, feed rate of 0.15 mm/rev and cutting depth of 0.3 mm. The highest value for nose radius of 0.8 mm is found as 322.33 N for the cutting speed of 150 m/min, feed rate of 0.15 mm/rev and cutting depth of 0.3 mm. The highest value for nose radius of 1.2 mm is obtained as 333.46 N for the cutting speed of 90 m/min, feed rate of 0.15 mm/rev and cutting depth of 0.3 mm.

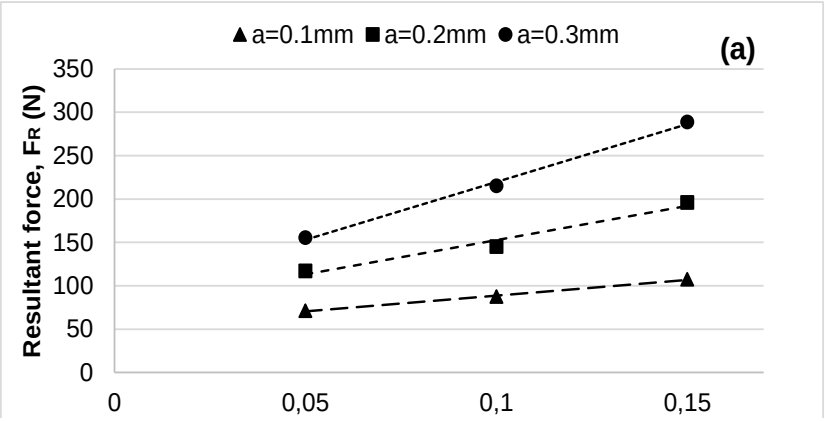

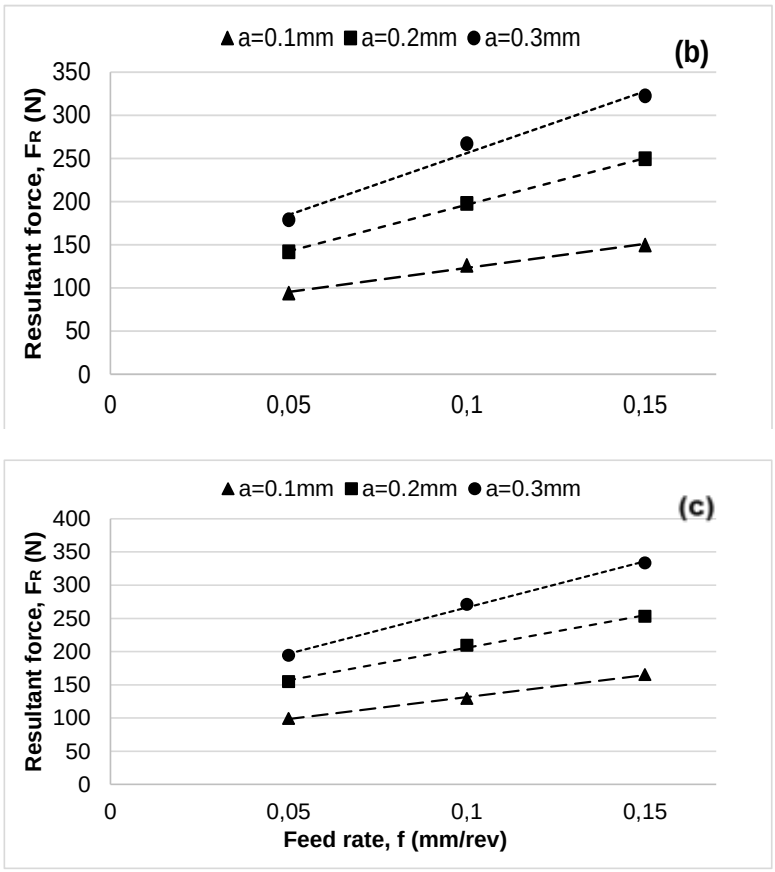

Figure 4 F_R results; a) r=0.4 mm. b) r=0.8 mm c) r=1.2 mm

Additionally, analysis of variance (ANOVA) results performed on the 95% confidence level in order to determine the effects of factors on the F_R are given in Table 3. Here, the probability (P) values indicating the importance level of each factor, degree of freedom (DF), the sum of squares (SS), mean square (MS), F values and the percent contribution ratio (PCR) is shown. P value should be lower than 0.05 in 95% confidence level in order to determine that any factor acting on the force is effective on it. Table 3 indicates that the most effective factor on the resultant force is depth of cut with 60.99 % PCR. The feed rate and tool nose radius have effect on resultant force with 27.71 % and 10.00 % PCR, respectively.

Table 3 ANOVA results for F_R

Factor	DF	SS	MS	F value	P value	PCR (%)
a	2	205.834	102.917	440.42	0.000	60.99
f	2	93.502	46.751	200.07	0.000	27.71
V	2	0.174	0.087	0.37	0.694	0.06
r	2	33.746	16.873	72.21	0.000	10.00
Error	18	4.206	0.234			1.24
Total	26	337.461				100.00

A total of 27 analyses including nine for each tool nose radius were done by using cutting forces obtained on experiments. Cutting tool stresses were examined according to changes of depth of cut, feed rate and cutting speed. The von Mises stress (S_{EQV}) variations are given in Fig. 5. When the graphs are generally examined, there is a different tendency on von Mises stress (S_{EQV}) for nose radius of 0.4 mm while those of 0.8 and 1.2 mm have similar tendency. The S_{EQV} values for all tool nose radius increase with increasing feed rate. However, von Mises stresses have not regular increase or decrease tendency with increasing depth of cut for nose radius of 0.8 and 1.2 mm while those of 0.4 mm increase with increasing depth of cut. This increasing tendency for tool nose radius of 0.4 mm may be referred to that increasing ratio on cutting forces is larger than increase on tool-chip contact area by depth of cut from 0.1 to 0.3 mm. The cutting tool stresses have a large decrease with increasing depth of cut from 0.1 to 0.2 mm for tool nose radius of 0.8 mm while there is a small increase on the stresses with increasing depth of cut from 0.2 to 0.3 mm. The tool nose radius of 1.2 mm has similar tendency with those of 0.8 mm nose radius.

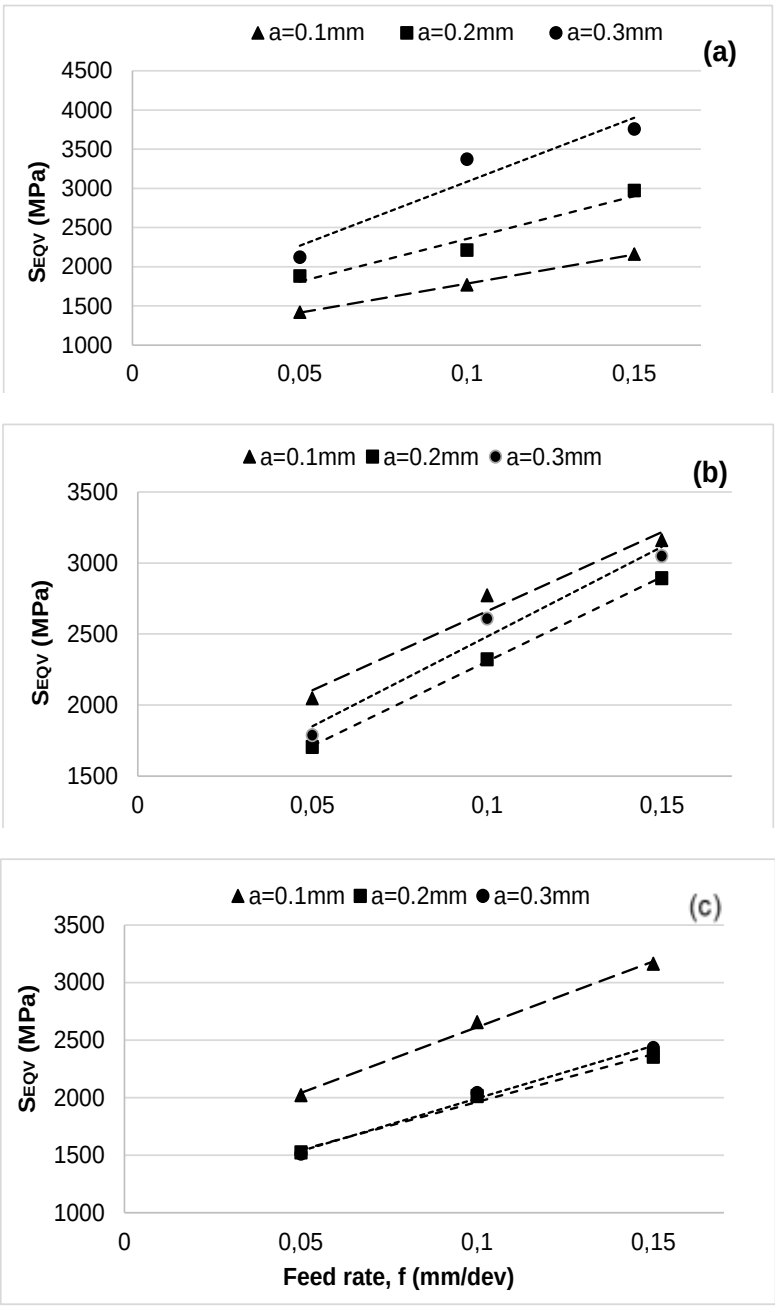

Figure 5 S_{EQV} results; a) r=0.4 mm. b) r=0.8 mm c) r=1.2 mm

The highest value for S_{EQV} is obtained as 3758 MPa for the cutting speed of 120 m/min, feed rate of 0.15 mm/rev, cutting depth of 0.3 mm and nose radius of 0.4 mm. The highest S_{EQV} value for nose radius of 0.8 mm is 3161 MPa for the cutting speed of 150 m/min, feed rate of 0.15 mm/rev, cutting depth of 0.1 mm. Finally, the highest value for cutting tool stresses is found as 3163 MPa for the cutting speed of 90 m/min, feed rate of 0.15 mm/rev, cutting depth of 0.1 mm and tool nose radius of 1.2 mm.

3.2 Evaluation of S_{EQV}

Von Mises stresses is achieved by using cutting forces in hard machining of AISI L2 tool steel with coated ceramic cutting tool. It is mentioned that wear zone on cutting tool may be forecasted according to von Mises stress distributions[21].

In this regard, stress analysis results for nose radius of 0.4 mm performed on ANSYS is shown in Fig. 6b. In addition, tool image (Fig. 6a) is taken from Nikon SMZ745T microscope in order to demonstrate the consistency of ANSYS results and locate the possible wear zone on cutting tool.

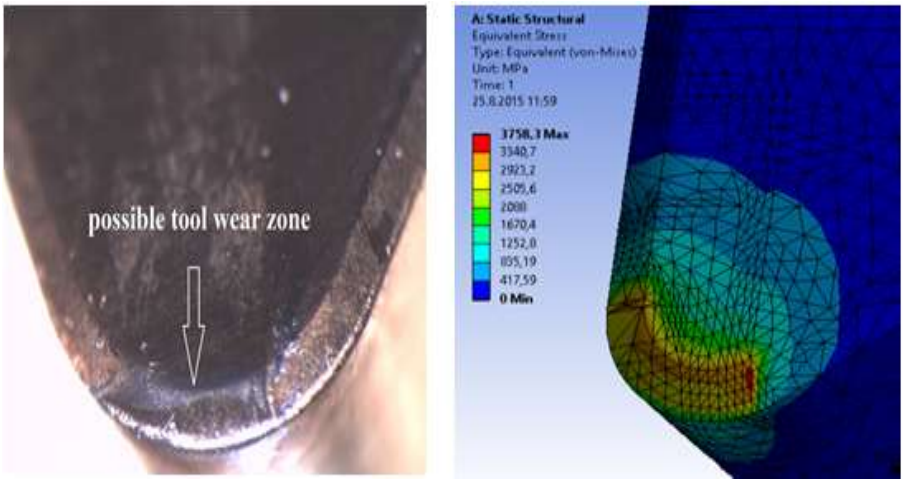

a) Microscope (x60) **b) ANSYS**

Figure 6 Cutting tool images (a=0.3mm, f=0.15mm/rev, r=0.4mm)

The apparent wear type was not observed at the coated ceramic tools during hard turning (Fig. 6a). However, von Mises stress distributions in cutting tool rake face provide information about probable tool wear zone occurred at tip of tool chip contact area when hard turning has been continued (Fig. 6b), as mentioned in Ref.[18]. In addition, the crater wear which is the most common damage type in hard turning may occur at the chamfered zone of tool-nose because of the fact that the cutting area is very small. Because, chamfered tool geometry causes negative rake angle and increase cutting forces, thus high cutting stresses occurred on tool-chip contact area. As can be seen from the Figure 6, cutting tool image taken from FEA and tool microscope are very similar. The model of tool-chip contact area and boundary conditions of applying cutting force components on this area is correct. Hence, it is possible to say that the prediction of von Mises stresses by finite element analysis and so the type of tool wear can be determined in hard tuning processes.

In the final stage of this study, reliability of mathematical model has been assessed with various error control methods in order to demonstrate the suitability of model. Due to fact that training and testing procedure in ANN has been performed by considering an error value (e), average of the sum of these error values is needed to be minimized. This minimized value is the mean squared error (MSE) that is a criteria determining the ANN performance. Root-mean-squared (RMS), coefficient of determination (R2), mean absolute percentage error (MAPE) has been taken into consideration as criteria in similarity between finite element analysis and ANN results.

$$MSE = \frac{1}{p}\sum_i {e_i}^2 = \frac{1}{p}\sum_i (t_i - o_i)^2 \quad (10)$$

$$RMS = \sqrt{MSE} = \sqrt{\frac{1}{p}\sum_i {e_i}^2} = \sqrt{\frac{1}{p}\sum_i (t_i - o_i)^2} \quad (11)$$

$$R^2 = 1 - \left(\frac{\sum_i (t_i - o_i)^2}{\sum_i {o_i}^2}\right) \quad (12)$$

$$MAPE = \frac{1}{p}\sum_i \frac{|t_i - o_i|}{t_i} \times 100 \quad (13)$$

In Eqns. 10-13, p, t_i, o_i and e_i show the sample experiment number, output value from experiments, output value from ANN and error value, respectively. The applicability of developed model increases when R^2 value approaches to 1.

Table 4 shows that mean absolute percentage error for S_{EQV} has been calculated as 1.84495 % in training results while it is 7.029301 % in testing results. The calculation of R^2 values as 99 % shows the reliability of ANN model for S_{EQV}. The comparison of S_{EQV} obtained from FEA and ANN results has been illustrated in Fig. 7. It is clearly seen that the S_{EQV} values are very close to each other. In addition, it is confirmed that the results of FEA and ANN have a linear relationship with 99 % coefficient of determination.

Table 4 The statistical error values for S_{EQV}.

	RMS	***R²***	***MAPE***
ANN Training Data	5.040597	0.999574	1.84495
ANN Test Data	16.65833	0.995559	7.029301

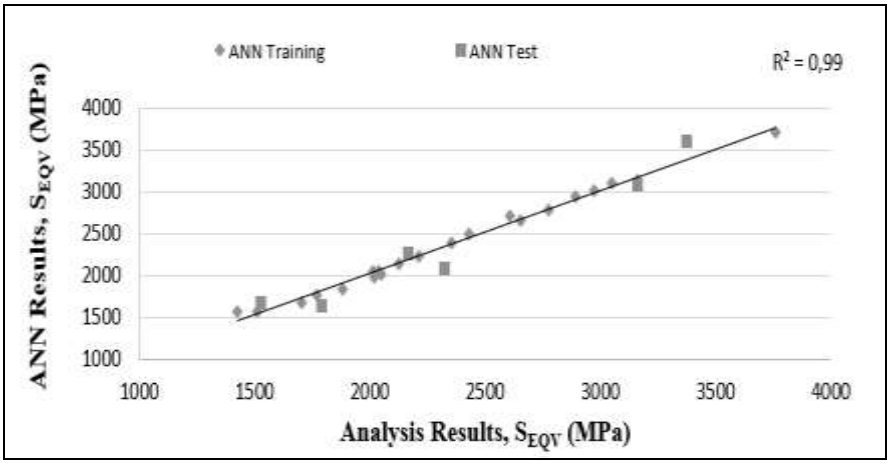

Figure 7 ANN performance for S_{EQV}

III. CONCLUSIONS

In this study, resultant cutting force and von Mises stress have been investigated in hard turning of AISI L2 steel workpieces with 60±1 HRC hardness using TiN coated mixed ceramic inserts. Von Mises stresses on cutting tool have also been analyzed with finite element method. Predictive mathematical model was developed by artificial neural network for von Mises stress. The following conclusions are drawn from this study:

1. The resultant cutting forces increased with increasing feed rate, depth of cut and tool nose radius. It was determined that F_R values increased 39 % with increasing of nose radius from 0.4 to 1.2 mm.
2. The most important factor on resultant cutting force is depth of cut with %60.99 PCR according to ANOVA results.
3. The results of FEA showed that von Mises stresses increased with increasing feed rate for all tool nose radius. In addition, von Mises stresses increased with increasing depth of cut with tool nose radius of 0.4 mm. However, the S_{EQV} decreased for other tool nose radius depending on that the increasing ratio on cutting forces is smaller than that on tool-chip contact area.
4. The highest value for S_{EQV} was obtained as 3758 MPa for the cutting speed of 120 m/min, feed rate of 0.15 mm/rev, cutting depth of 0.3 mm and tool nose radius of 0.4 mm.
5. The predictive modelling results indicated that 3% deviation was calculated between FEA and ANN results. Hence, this study confirmed that the prediction of von Mises stresses by finite element analysis and so the type of tool wear can be determined in hard tuning processes.
6. FEA results showed that the boundary conditions for loading of cutting forces are correct and the prediction of cutting tool stresses statically by finite element analysis can be determined in hard tuning processes.

REFERENCES

[1]. H.K. Tonshoff, C. Arend, R.B. Amor, Cutting of hardened steel, CIRP Ann Manuf Technol, 49(2) (2000), 547–566.
[2]. F. Hashimoto, Y.B. Guo, A.W. Warren, Surface integrity difference between hard turned and ground surfaces and its impact on fatigue life, CIRP Ann Manuf Technol, 55(1) (2006) 81–84.
[3]. Y. Huang, Y.K. Chou, S.Y. Liang, CBN tool wear in hard turning: a survey on research progresses, Int J Adv Manuf Technol, 35 (2007) 443–453.
[4]. T.G. Dawson, T.R. Kurfess, Modeling the Progression of Flank Wear on Uncoated and Ceramic-Coated Polycrystalline Cubic Boron Nitride Tools in Hard Turning, J. Manuf. Sci. Eng 128(1) (2004) 104-109.
[5]. R. Suresh, S. Basavarajappa, V.N. Gaitonde, G.L. Samuel, Machinability investigations on hardened AISI 4340 steel using coated carbide insert, Int J Refract Metals Hard Mater, 33 (2012) 75–86.
[6]. H. Aouici, M.A. Yallese, K. Chaoui, T. Mabrouki, J.F. Rigal, Analysis of surface roughness and cutting force components in hard turning with CBN tool: Prediction model and cutting conditions optimization, Measurement, 45 (2012) 344-353.
[7]. V.N. Gaitonde, S.R. Karnik, L. Figueira, J.P. Davim, Machinability investigations in hard turning of AISI D2 cold work tool steel, Int J Refract Metals Hard Mater, 27 (2009) 754-763.

[8]. S. Chinchanikar, S.K. Choudhury, Effect of work material hardness and cutting parameters on performance of coated carbide tool when turning hardened steel: An optimization approach, Measurement, 46 (2013) 1572-1584.
[9]. B. Karpuschewski, K. Schmidt, J. Beno, I. Manková, J., Prilukova, Measuring procedures of cutting edge preparation when hard turning with coated ceramics tool inserts, Measurement, 55 (2014) 627-640.
[10]. M. Sokovic, B. Barisic, S. Sladic, Model of quality management of hard coatings on ceramic cutting tools, J Mater Process Technol, 209 (2009) 4207–4216.
[11]. A.K. Bhattacharya, K. Zimmermann, G.A. Schneider, W. Hintze, Influence of surface modification on the cutting performance of reaction–sintered Al2O3–TiOC ceramics, J Am Ceram Soc, 91(9) (2008) 2982–2986.
[12]. L. Chen, T.I. El-Wardany, M. Nasr, M.A. Elbestawi, Effects of edge preparation and feed when hard turning a hot work die steel with polycrystalline cubic boron nitride tools, CIRP Ann Manuf Technol, 55(1) (2006) 89–9213.
[13]. L. Malecek, M. Fedorko, F. Vancura, H. Jirková, B. Masek, Development of numerical models for the heat-treatment-process optimization in a closed-die forging production, Mater Technol, 49(3) (2015) 471-475.
[14]. M. Duchek, T. Kubina, J. Hodek, J. Dlouhy, Development of the production of ultrafine-grained titanium with the conform equipment, Mater Technol, 47(4) (2013) 515-518.
[15]. H. Yan, J. Hua, R. Shivpuri, Flow stress of AISI H13 die steel in hard machining, Mater Design, 28(1) (2007) 272-277.
[16]. D. Umbrello, S. Rizzutia, J.C. Outeiro, R. Shivpuri, R. M'Saoubi, Hardness-based flow stress for numerical simulation of hard machining AISI H13 tool steel, J Mater Process Technol, 199(1-3) (2008) 64-73.
[17]. T. Özel, Computational modelling of 3D turning: Influence of edge micro-geometry on forces, stresses, friction and tool wear in PcBN tooling, J Mater Process Technol, 209(11) (2009) 5167–5177.
[18]. T. Özel, A. Nadgir, Prediction of flank wear by using back propagation neural network modeling when cutting hardened H13 steel with chamfered and honed CBN tools, Int J Mach Tool Manuf, 42(2) (2002) 287–297.
[19]. D. Umbrello, G. Ambrogioa, L. Filice, R. Shivpuri, An ANN approach for predicting subsurface residual stresses and the desired cutting conditions during hard turning, J Mater Process Technol, 189(1-3) (2007) 143–152.
[20]. X. Wang, W. Wang, Y. Huang, N. Nguyen, K. Krishnakumar, Design of neural network-based estimator for tool wear modeling in hard turning, J Intell Manuf, 19 (2008) 383-396.
[21]. A. Kurt, B. Yalçin, N. Yilmaz, The cutting tool stresses in finish turning of hardened steel with mixed ceramic tool, Int J Adv Manuf Technol, 80 (2015) 315-325.
[22]. N.N. Zorev, Inter-relationship between shear processes occurring along tool face and shear plane in metal cutting. In International Research in Production Engineering, Proceedings of the International Production Engineering Research Conference, (1963) 42–49.
[23]. A. Toropov, S.L. Ko, Prediction of tool-chip contact length using a new slip-line solution for orthogonal cutting, Int J Mach Tool Manuf, 43 (2003) 1209–1215.
[24]. M.E. Korkmaz, Modeling of cutting tool stresses on machining of hardened cold work tool steel", MSc. Thesis, University of Karabük, (2015) 56.
[25]. T. Özel, Y. Karpat, Predictive modeling of surface roughness and tool wear in hard turning using regression and neural networks, Int J Mach Tool Manuf, 45(4-5) (2005) 467-479.